AD-A155 227   APPLIED RESEARCH AND DEVELOPMENT FOR FALLING-SPHERE AIR   1/1
DENSITY MEASURING SYSTEMS(U) ACCUMETRICS CORP ROCKPORT
MS D H FRYKLUND AUG 84 AFGL-TR-84-0192

UNCLASSIFIED   F19628-81-C-0050   F/G 14/2   NL

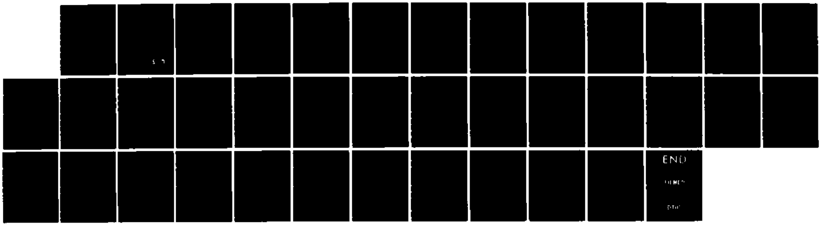

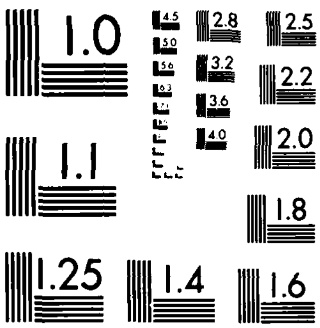
1.0
4.5
5.0
5.6
6.3
2.8
3.2
3.6
4.0
2.5
2.2
2.0
1.1
1.8
1.25
1.4
1.6

(7)

AFGL-TR- 84-0192

AD-A155 227

APPLIED RESEARCH AND DEVELOPMENT FOR FALLING-SPHERE AIR DENSITY MEASURING SYSTEMS

Donald H. Fryklund

Accumetrics Corporation
Frank Street
Rockport, Massachusetts 01966

August 1984

Final Report for period 81 January to 84 August

AIR FORCE GEOPHYSICS LABORATORY
AIR FORCE SYSTEMS COMMAND
UNITED STATES AIR FORCE
HANSCOM AFB, MASSACHUSETTS 01731

This technical report has been reviewed and is approved for publication.

JOSEPH P. MCISAAC
Contract Manager

ROBERT W. FENN
Branch Chief

FOR THE COMMANDER

JOHN S. GARING
Division Director

This report has been reviewed by the ESD Public Affairs Office (PA) and is releasable to the National Technical Information Service (NTIS).

Qualified requestors may obtain additional copies from the Defense Technical Information Center. All others should apply to the National Technical Information Service.

If your address has changed, or if you wish to be removed from the mailing list, or if the addressee is no longer employed by your organization, please notify AFGL/DAA, Hanscom AFB, MA 01731. This will assist us in maintaining a current mailing list.

unclassified

SECURITY CLASSIFICATION OF THIS PAGE (When Data Entered)

REPORT DOCUMENTATION PAGE		READ INSTRUCTIONS BEFORE COMPLETING FORM
1. REPORT NUMBER AFGL-TR-84-0192	2. GOVT ACCESSION NO. AD-A155227	3. RECIPIENT'S CATALOG NUMBER
4. TITLE (and Subtitle) APPLIED RESEARCH AND DEVELOPMENT FOR FALLING-SPHERE AIR DENSITY MEASURING SYSTEMS		5. TYPE OF REPORT & PERIOD COVERED Final Report January 1981 - August 1984
		6. PERFORMING ORG. REPORT NUMBER
7. AUTHOR(s) Donald H. Fryklund		8. CONTRACT OR GRANT NUMBER(s) F19628-81-C-0050
9. PERFORMING ORGANIZATION NAME AND ADDRESS Accumetrics Corporation Frank Street Rockport, Massachusetts 01966		10. PROGRAM ELEMENT, PROJECT, TASK AREA & WORK UNIT NUMBERS 62101F 669004AP
11. CONTROLLING OFFICE NAME AND ADDRESS Air Force Geophysics Laboratory Hanscom AFB, Massachusetts 01731 Monitor: Joseph P. McIsaac/C. R. Philbrick/LKB		12. REPORT DATE August, 1984
		13. NUMBER OF PAGES 39
14. MONITORING AGENCY NAME & ADDRESS(if different from Controlling Office)		15. SECURITY CLASS. (of this report) Unclassified
		15a. DECLASSIFICATION/DOWNGRADING SCHEDULE

16. DISTRIBUTION STATEMENT (of this Report)

Approved for public release; distribution unlimited

17. DISTRIBUTION STATEMENT (of the abstract entered in Block 20, if different from Report)

18. SUPPLEMENTARY NOTES

19. KEY WORDS (Continue on reverse side if necessary and identify by block number)

Piezoelectric
Accelerometer
Transducer
Densitometer
Atmospheric Density

20. ABSTRACT (Continue on reverse side if necessary and identify by block number)

Four complete falling-sphere densitometer systems were designed and fabricated and were launched at four locations: Wallops Island, VA; Kiruna, Sweden; Poker Flat, Alas.; and Andoya, Norway. The former back-up densitometer was upgraded and was flown during the Norway program. Three unique support units were designed and fabricated for use with the European payloads. A solar aspect system was designed, fabricated and flown on the Alaskan payload. Additionally, several studies were performed to generally improve the ground and flight equipment.

DD FORM 1 JAN 73 1473

unclassified

SECURITY CLASSIFICATION OF THIS PAGE (When Data Entered)

FOREWORD

This document is the final report required under Contract No. F19628-81-C-0050 to perform engineering research and development to evolve, fabricate, test, and launch falling-sphere densitometer payload systems of improved design.

Acknowledgement

The author wishes to acknowledge the efforts of several administrators, scientists, engineers, and technicians who have supported and contributed to the success of the Ten-inch Piezo-electric Falling-sphere Air Density Research Program over the many years of its development and utilization.

Recognized and appreciated are the encouragement and contributions of Dr. KSW Champion who conceived the falling-sphere program, of Mr. A.C. Faire whose unfailing support of the development during its early difficulties is greatly appreciated, and of Mr. Vic Corbin for his evaluation of the system, and for his recognition of the merits of the system.

In particular, acknowledgement and appreciation are extended to Dr. C.R. Philbrick for his contributions and whose excellent data studies revealed additional high altitude atmospheric data not sought in the initial program. Greatly appreciated are the efforts of Mr. W. Mustoe who steadfastly developed the system electronics, assembled the systems, and assisted in the testing and fielding of the final payloads. Finally, the contribution of Mr. J. P. McIsaac is acknowledged for his fair and objective monitoring of the program.

TABLE OF CONTENTS

LIST OF FIGURES

NOMENCLATURE

a	Acceleration, instantaneous
A	Acceleration, peak or steady state
A	Constant
B	Constant
C	Capacitance, farads, microfarads
d	Distance
E	Emf, volts
F	Force
f	Frequency, Hz
f_n	Natural frequency, Hz
g	Acceleration due to gravity
K	Spring constant
K	Constant of proportionality
K	Gain
L	Length
m	Mass
R	Resistance, ohms
R	Radius
r	Radius
t	Time, seconds
T	Tolerance
T	Time constant
V	Voltage, volts, or velocity
V_0	Voltage, output, volts
W	Energy
x	Distance, instantaneous
X	Distance, steady state
ω	Frequency, angular velocity, radians/second
ω_n	Natural angular frequency, zero-g
ω_{nT}	Natural angular frequency, Test, sea level
ω_{ns}	Natural angular frequency, Flight
ω_s	Spin angular frequency

I. INTRODUCTION

1.0 General

The subject contract involves the development, fabrication, testing, and calibration of four complete high altitude densitometer payloads, each comprised of a nose cone, an ejection system, and a ten-inch falling sphere. The sphere, in turn, is instrumented with a sensitive accelerometer, a TM system (GFE), a nutation sensor, and various ancillary power supply and control systems.

Air density is determined by measuring the negative air-drag acceleration as experienced by the sphere as it falls through the atmosphere. By evaluating the air drag equation for a spherical shape having the same area and mass, with the measured fall velocity and negative acceleration the air density profile for the trajectory can be calculated. Air density measurement over the desired range of 50 to 150 KM requires the use of a sensitive accelerometer having a dynamic range of 10^{-2} to 10^{-7} g's.

The feasibility of reaching a low measuring threshold such as 10^{-7} g's is enabled by several factors inherent in the falling sphere system and its environment, and by advances in semiconductor state-of-the-art. The air drag acceleration on the falling sphere is essentially a slowly varying exponential quality whose measurement would normally require a force-balance type of accelerometer. However, since the launch vehicle for the experiment is spin-stabilized the sphere acquires a known spin at ejection which, in effect, modulates or chops the drag acceleration as seen by the on-board accelerometer. Therefore, an A.C. type piezoelectric accelerometer devoid of drift problems may be used to measure the drag acceleration. Additionally, the absence of earth gravity in the free-falling sphere environment enables sensitivity maximization by the use of large seismic

masses in the instrument design. Hazard to crystal fracture at sea level due to the large mass load in the one-g field is eliminated by clamping or caging the mass until ejection during free-fall. Finally, the development of the low noise field-effect transistors has enabled the achievement of low electrical noise levels at the input to the transducer amplifier.

The task of integration includes the configuration of all payload subsystems into the sphere, the fabrication of secondary structure, wiring, static balancing, moment-of-inertia adjustment, and electrical testing.

Because of the unavoidable dispersion of the seismic mass centers of the accelerometer about the vehicle mass center, the instrument will sense body motion acceleration. This motion is in the form of a nutation or free precession of the spinning sphere whose frequency can be controlled by trimming the principle moments-of-inertia. The frequency of nutation is set to a convenient position in the data spectrum where the unwanted acceleration can be removed by the use of band-rejection filters.

Included in each sphere system is a wide-band accelerometer system comprised of a single-axis piezoelectric accelerometer aligned with the Z or spin axis which will enable the measurement of high altitude winds and turbulences of finer structure than is capable of measurement by the main accelerometer system.

Former rocket flights of the ten-inch falling sphere densitometer utilized a separate support unit comprised of various sensors to monitor the performance of the rocket spin, acceleration, burn times, and separation events. These data were telemetered to the ground via a separate TM link. It was observed during early flights that the sphere TM link fed by the various accelerometers on board the sphere was duplicating these data and that considerable cost savings would be realized by the elimination of the

additional sensors and support TM unit and, instead, provide a simple unit, or a mini-support unit, which would provide only the bare necessities to perform the nose cone and sphere ejection functions.

1.1 Subject Program

The objective of the subject program was to provide additional falling-sphere densitometers of improved design for various aeronomy rocket campaigns in Europe and the USA. Instrumentation variations in ancillary equipment were provided to adapt the payloads to specific flights. Four new systems were designed, fabricated, tested and launched. Additionally, a fifth system, which was formerly a back-up unit, was upgraded, tested, and launched.

Three support units, which were located immediately aft of the densitometer payloads on the rocket build-up and which provided pyrotechnic power, timing, and switching, were fabricated, tested and launched to service three of the densitometer systems.

The block-house control consoles were re-furbished to include new battery chargers for the ground charging of the pyrotechnic power packs in the payload support units. A special eighty-foot umbilical cable was fabricated for use at the Wallops Island launch facility.

To facilitate the examination of instantaneous acceleration data, a solar sensor was designed, fabricated, and tested. This system, installed on one densitometer, provided spin phase reference during flight.

To ... e the accuracy of the transducer calibration system, a standard accelerometer s designed and built. This unit was calibrated by the use of a microsc .e having a precision reticle. A comparator system comprised of two amplif ers was designed and built: one having unity gain and the other having variable gain. Their outputs fed an adding circuit, and their inputs were fed by the transducer under test, and the standard accelerometer, respectively, thus enabling the nulling of their combined outputs. The

$$f = F_0 \sin \omega t$$

generated by the E-M exciter. F_0 is of no concern in the procedure except that it should be of the required amplitude to generate a noise-free displacement X.

5.2 Calibrator-mounted Response of the Transducer Assuming Ideal Rigidity of Mounting

The dynamical case representing the calibration system is shown on P. 183 of W.T. Thomson, Vibration Theory and Applications, Prentice-Hall, 1965. The solution of this case in the text demonstrates the reaction of the spring-mass system comprised of k_2 and m_2 on the displacement of m_1. For example, at resonance of k_2 and m_2 the displacement of m_1 is reduced to zero. Because in the calibration case the displacement of X_1 is maintained constant by varying the forcing function, given above, only certain parts of this solution is pertinent.

The equation b-2, P. 183, op cit, is the equation of motion for k_2 and m_2 which in this case is the transducer

$$m_2 \ddot{x}_2 = -k_2 (x_2 - x_1) \qquad \text{b-2 (op cit).}$$

Because the transducer response is an analog voltage generated by the strain in the spring (bimorph) a parameter

$$z = x_2 - x_1 \qquad 1.$$

is used which represents the variation in length of the spring k_2 (or the strain in the spring). Also, from Equation 1, it follows that

$$\ddot{z} = \ddot{x}_2 - \ddot{x}_1 \qquad 2.$$

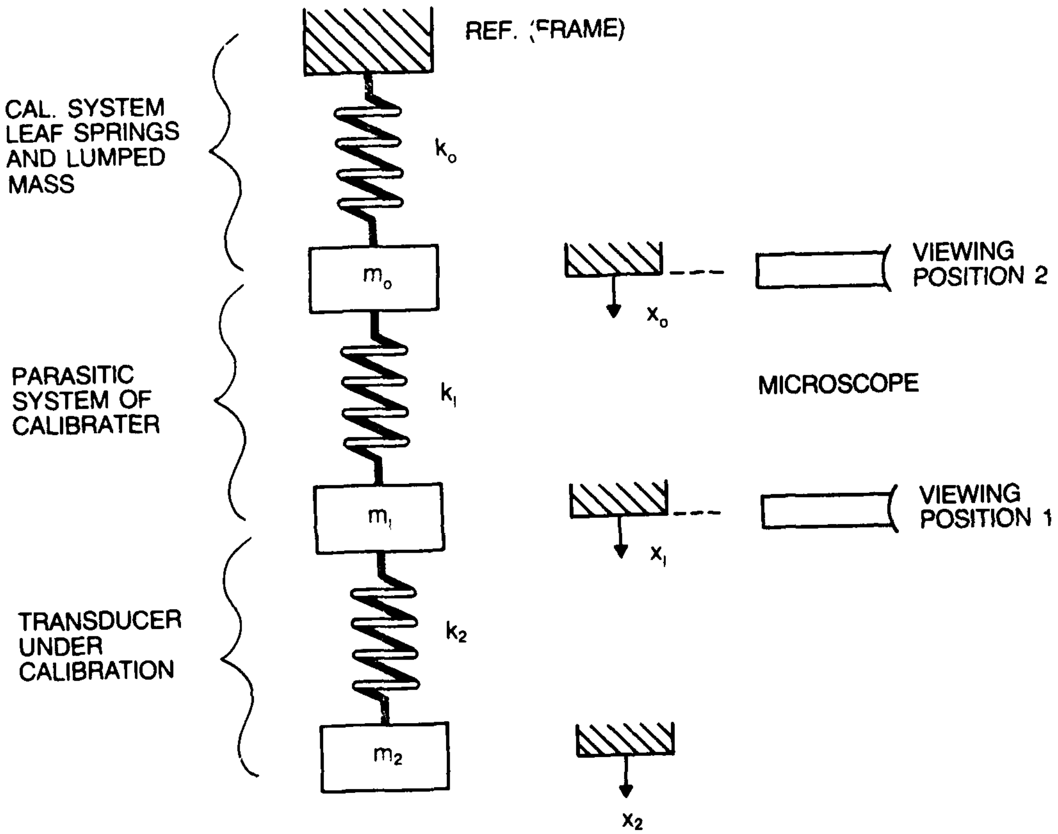

CALIBRATION SYSTEM SCHEMATIC

FIGURE 3

5.1 System Description

Figure 3 is the schematic of the dynamic parameters of the calibration system including the transducer. From top to bottom, the cross hatching is the stationary frame structure and reference for the observed motions of the system. k_o is the spring constant of the long flexible leaf spring supports of the armature of the calibrator and m_o is the lumped mass of the armature. x_o is the displacement of m_o, the parameter, k_1 is the spring constant of the distributed compliance of the attachment end of the armature, and m_1 is the distributed mass of the attachment end of the armature. These parameters, k_1 and m_1, comprise the subject parasitic mode. x_1 is the displacement of m_1. The parameters k_2 and m_2 represent the spring constant and mass of the transducer being calibrated, and x_2 is the displacement of the transducer mass, m_2.

Viewing position No. 1 was initially assumed to be valid, that is, that the true base of the transducer was being observed. The study revealed that the viewing position was in fact at position No. 2. It should be noted that in the derivation of the dynamical equation, the parameters above the viewing position (or assumed input excitation base) will be outside the system and will not appear as controlling quantities.

The calibration procedure, as is described in detail in earlier reports by the author, involves the generation of a measurable sinewave displacement of the armature (observable by use of the microscope) at a known frequency and by evaluating the equation

$$\ddot{X} = \omega^2 X \sin \omega t$$

where X is the displacement observed with the microscope. This is adjusted to measurable amplitude by varying the forcing function

V. CALIBRATION SYSTEM PARASITIC-OSCILLATION-MODE STUDY

5.0 General

The foregoing is a discussion of the results of an investigation initiated to determine a small systematic variation in a parameter which should theoretically be a constant-of-proportionality in the calibration of data of the main accelerometer transducers. This parameter was found to be a function of frequency of the sinewave forcing function when the dynamical equation for the transducer was assumed to be a base-excited single-degree-of-freedom system. This assumption was deemed valid because in the design of the transducers the mass and compliance were highly concentrated, or lumped, the mass being very large and stiff and the spring (bimorph) being very low in mass and very compliant. This defined the desired low frequency oscillation mode and placed secondary or parasitic modes at very high frequencies thus having negligible affect on the transducer response at its normal operating frequency. The assumption of base excitation means that the input acceleration is measured at the true base or attachment point of the transducer. It was found that this measuring point was not at the true base of the transducer, and that the calibration system introduced another oscillation mode between the reference point and the base of the transducer thus requiring the assumption of a dynamical representation for the calibration process having base excitation but with two degrees-of-freedom.

The study therefore evolved correction factors for adjusting prior calibration data and suggested the modification of the calibration system to remove the parasitic oscillation mode so the more simple and therefore more accurate dynamical representation as originally assumed would be valid.

The output of the system was useable over a total angle of 45 degrees ($\pm$ 22.5 degrees from normal), and was in the form of a trapezoid having some small irregularities on its top but having well-defined leading and trailing sides. The irregularities were attributed to find scratches on the end of the glass fiber.

Limitations in the precision of the protractor system did not allow examination of the full capabilities of the system but repeated measurements indicated that the determination of the sun ray with respect to the sphere fixed axes would be within one degree, and differences in angle from one spin cycle to the next would be more precise, possibly by a factor of ten. The latter was speculation as the calibration system could not be read to these very small angles.

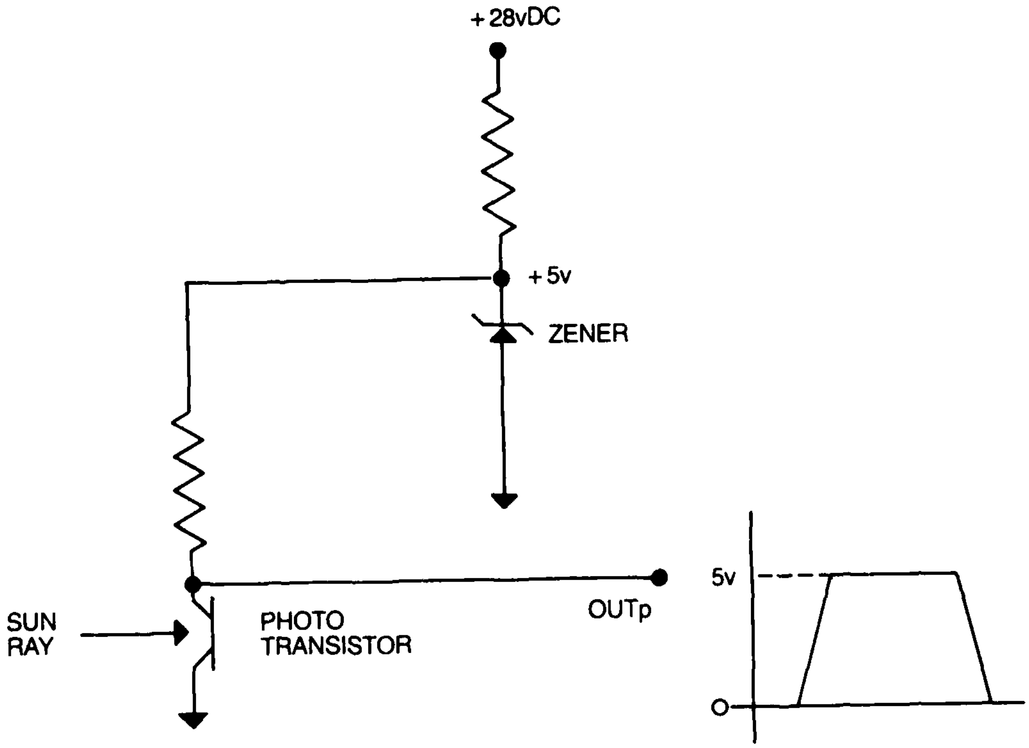

SOLAR SENSOR SCHEMATIC

FIGURE 2

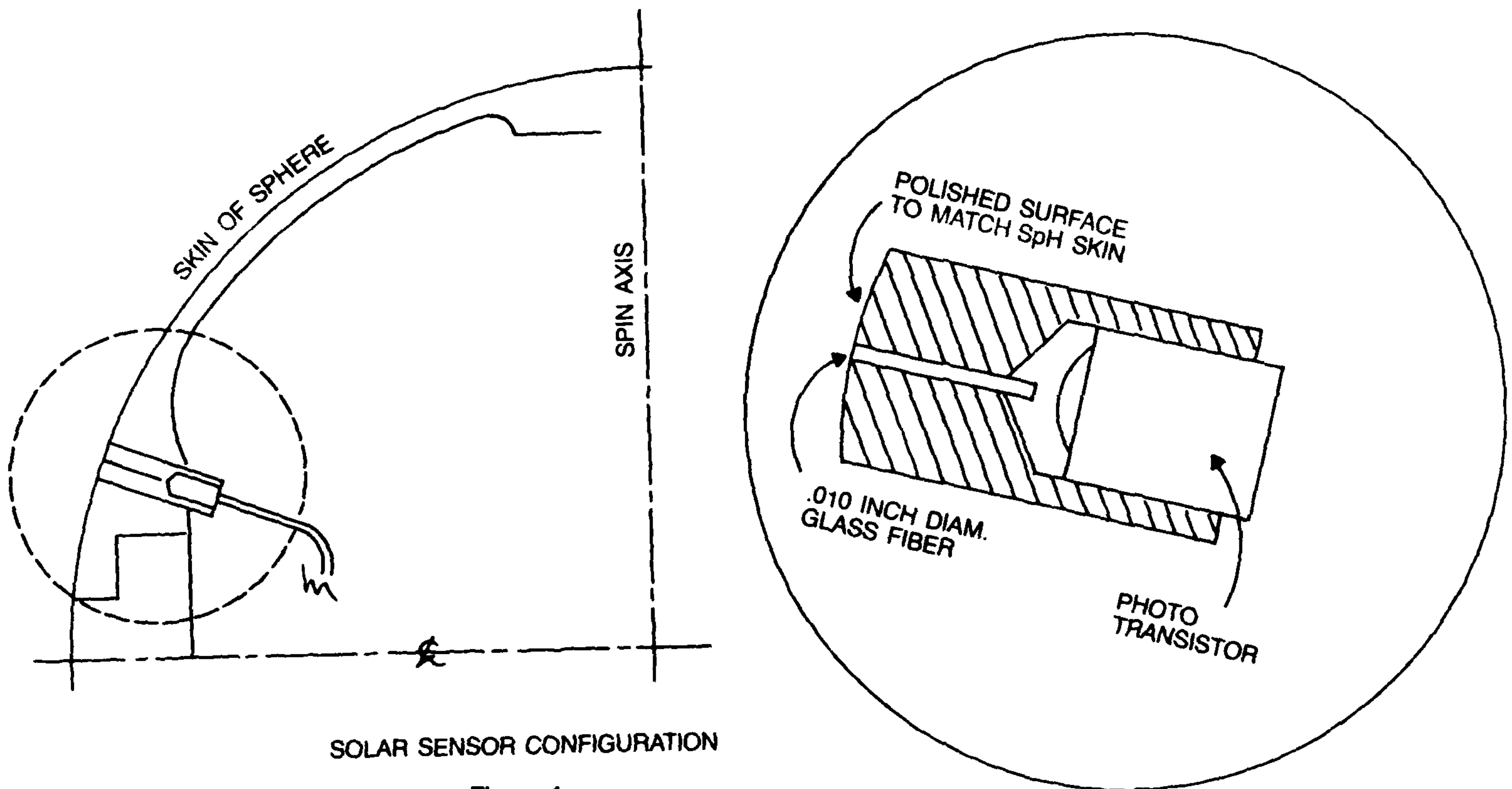

SOLAR SENSOR CONFIGURATION

Figure 1

of the sensor was approximately 45 degrees.

4.2 Sensor Design

In order not to alter the polished surface of the sphere and therefore to prevent asymmetrical drag torque, the sun illumination was transmitted through the skin of the sphere by a single 0.010-inch diameter glass fiber. This fiber was installed in a cylindrical housing which contained a photo transistor. This assembly was fitted into a socket precisely drilled radially from the inside of the upper end-cap at an angle of 30 degrees from the sphere spin-plane. A small hole was then provided through the skin for egress of the fiber. After assembly the fiber was cut off flush with the skin and polished smooth with rouge to provide an efficient optical surface. This detail is depicted in Figure 1. Since the sensor was to provide only angular information without concern for amplitude calibration, it was determined that a very simple circuit would be sufficient. This circuit is shown in the schematic of Figure 2. It was found that zener diode voltage reulation of the 28-volt buss supply would provide ample stability while at the same time would provide for the 0-to-5 volt clamping required by the TM input.

4.3 Calibration

The solar angular aspect system was tested and calibrated by suspending the sphere vertically by the use of nylon cords, one above and one below the sphere, to enable it to be rotated about its spin axis. The apparatus was moved outdoors on a bright, cloudless day, and a mirror was mounted onto a tripod rigged with a protractor to direct the sunrays at various angles onto the sphere. The sphere was rotated, and the sensor output was observed on a recorder.

IV. SOLAR ANGULAR ASPECT SENSOR

4.0 General

In the course of the Ten-inch Falling Sphere Program, it was discovered by C. Philbrick, et al, that the air drag vector as seen by the spinning sphere did not always lie in the plane of the trajectory as was normally expected, but, instead, moved in a systematic manner in and out of this plane. This was attributed to the affect of winds at various altitudes.

In order to study these wind affects, it was found that the shift in the phase of the spin-generated sinewave of acceleration must be accurately determined for successive spin cycles. To facilitate this phase measurement, a solar angular aspect sensor was designed, fabricated, tested, and installed on the densitometer Serial No. AC-17, which was scheduled for a mid-day flight at Poker Flat, Alaska during June 1983.

4.1 View-angle Geometry

The latitude at Poker Flat is approximately 65 degrees north which defines the noon sun-ray angle at the equinox as 25 degrees above the local horizon. In June, near the time of summer solstice, the earth will be tilted into the ecliptic toward the sun by an additional 23.5 degrees giving a local noon-time sun-ray elevation angle of 48.5 degrees. The rocket was to be launched in a northerly direction with approximately an eighty degree elevation angle, or 10 degrees off of vertical away from the sun. Thus, the sun ray as seen by the sphere would be 38.5 degrees above its spin plane, or would be normal to a point on its upper end-cap.

The sensor was then located at a convenient structural position which placed it approximately 30 degrees above the spin-plane viewing through the upper end-cap. This was deemed satisfactory since the field of view

The sphere was then pressure tested and brought to the AFGL shaker facility for vibration and shock testing. These tests involved the usual pre-shake, shake, and post-shake electronic system checks.

III. REFURBISHMENT OF BACK-UP DENSITOMETER

3.0 General

Densitometer Serial No. AC-8, which for prior programs was used for an emergency back-up payload was upgraded and was flown as one of the prime payloads participating in the MAPWINE Campaign at Andoya, Norway, during the winter 1983-84.

3.1 Refurbishment

The sphere was completely dis-assembled including the main accelerometer. All components and subsystems were examined and cleaned. A new deck was fabricated to accommodate the required configuration changes. The transducers from the main accelerometer were examined under a microscope for micro-cracks and electrode integrity. The external skin of the sphere segments was polished.

3.2 Component and Subsystem Replacement

The eight-bit encoder was replaced by a new ten-bit encoder (GFE). The older model radar beacon was replaced by a smaller updated model (GFE). The battery pack which had logged considerable cycle and shelf time was refurbished with new cells. A new set of O-ring seals was installed.

3.3 Calibration, Balancing and Testing

All Transducers of the main accelerometer, the wide band accelerometer, and the nutation sensor, were re-calibrated, as were all the amplifiers associated with these transducers. The accelerometers were then re-assembled and were mounted into the sphere structure. The main accelerometer was bore-sighted to bring its sensing center to coincidence with the geometric center of the sphere. The sphere systems were then re-wired. The completed sphere was statically balanced, and its moments-of-inertia were trimmed to achieve the desired spin dynamics.

Serial No. AC-17 comprised of a ten inch sphere implemented with a solar angular aspect sensor, nose cone, sphere-ejection system and a launcher umbilical.

Serial No. AC-18 comprised of a ten-inch sphere, nose cone, sphere ejection system, mini-support unit, and a launcher umbilical.

Serial No. AC-8 comprised of the refurbished and upgraded back-up ten-inch sphere, but with a newly fabricated nose cone, sphere ejection system, and mini-support unit. The umbilical for No. AC-18 was used for this payload.

II. DELIVERED END-ITEMS

2.0 General

The subject effort required the delivery of four complete densitometer falling-sphere systems. Three of these systems required support systems (mini-support units). One system required the implementation of an angular solar aspect sensor. A fifth complete densitometer was required in the form of a refurbished and upgraded back-up unit which was fabricated under an earlier program. The last two items are discussed under separate headings in this report. All systems required special launcher-block-house cabling and launcher umbilicals. Delivered but not in the specifications were two battery chargers for launch-pad charging of the pyro batteries. These units were incorporated into the block-house launch consoles.

The fabrication, testing, and calibration of the various required accelerometers; the fabrication, integration, bore-sighting, balancing, second-moment adjustment, and testing of the ten-inch spheres; the fabrication and testing of the mini-support units, the nose cones, and ejection systems have been described in previous AFGL technical reports by the author. These reports are available at the AFGL library (and other technical libraries) under the author's name and under the key headings listed in Block 19 of DD Form 1473 page i of this report.

2.1 List of Delivered End-items

Five densitometer systems were delivered during the reporting period:

Serial No. AC-15 comprised of a ten-inch sphere, nose cone, sphere ejection system and launcher umbilical.

Serial No. AC-16 comprised of a ten-inch sphere, nose cone, sphere ejection system, a mini-support unit and a launcher umbilical.

standard sensitivity multiplied by the null-value of amplifier gain then gave a precise calibration of the test sample.

Studies were performed on the total system to determine the source of certain extraneous noise signals in the flight data and inconsistencies in the calibration data. The latter effect was determined to be caused by parasitic oscillation modes in the transducer motion generator used in the calibration process. The structure of this device was therefore re-designed to provide greater stiffness. Correction equations were then derived to enable the adjustment of data obtained from the former less-stiff system.

In the interest of the continued accuracy improvement of the calibration process, a special temperature chamber was built. This enabled the re-examination of all system components to determine temperature sensitivity.

A study was performed on the event-timer system used to generate discretes for nose-tip and sphere ejection to determine the most reliable cost-effective system to replace the mechanical timers presently used, and which are being phased out of production by the vendor.

Launch support was provided for four programs: Wallops Island, Virginia, in June 1982; Kiruna, Sweden, in July 1982; Poker Flat, Alaska, in June 1983; and Andoya, Norway, in December 1983.

Thus, Equation b-2 becomes:

$$m_2 \ddot{z} + m_2 \ddot{x}_1 = k_2 z$$

$$m_2 \ddot{z} - k_2 z = - m_2 \ddot{x}_1 \qquad 3.$$

It is seen that Equation 3 is the same as Equation 3.11-2 of page 75 (op cit) (C being small and negligible).

Noting that Y is replaced by X,

and X is replaced by X_2,

and that X is assumed to be the observed base motion (Viewing-Position No. 1 in the figure),

one obtains the single-degrees-of-freedom solution (neglecting the damping term which is small) Equation 3.11-4:

$$z = \frac{x_1 (\omega / \omega_{22})^2}{1 - (\omega / \omega_{22})^2}$$

or the transducer sensitivity function

$$\frac{V}{a} = S_s = \frac{K_s}{\omega_{22}^2 (1 - \omega^2 / \omega_{22}^2)} \qquad 3a.$$

5.3 <u>Calibrator-mounted Response of the Transducer for Non-rigid Mounting</u>

It is seen from the foregoing that if the dynamical model Figure 3 is a true representation of the system the observed transducer response should be that for a single-degree-of-freedom system.

The observed results, however, showed that the transducer response departed from a single spring-mass system by approximately 2.5 percent when ω / ω_N is varied from approximately 0.42 to 0.542.

It was apparent that the armature and/or the transducer mounting fixture at the end of the armature was flexing. Thus the actual displacement at the transducer was different by a small amount from the displacement measured at Position No. 2 of the armature where the microscope was located. This would place a spring-mass system k_1 and m_1 between the transducer and the point of observed acceleration. The observation point therefore should be located at Position No. 2, thus observing the displacement X_0.

The dynamical equations for the system then become

$$m_1 \ddot{x}_1 = k_2(x_2 - x_1) - k_1(x_1 - x_0) \qquad 4.$$

$$m_2 \ddot{x}_2 = -k_2(x_2 - x_1) \qquad 5.$$

When the system is excited, the motion at the point of observation will be

$$x_0 = X \sin \omega t$$

Equation 4 will then become

$$m_1 \ddot{x}_1 = k_2(x_2 - x_1) - k_1 x_1 + k_1 X_0 \sin \omega t$$

which is the same as Equation (b-1) on p. 183 (op cit).

Thus Equations 4 and 5 are identical to Equations (b-1) and (b-2) on page 183 (op cit) and are solved according to Equations (b-5) and (b-6) ensuing on p. 183.

The output of the transducer is, again, proportional to the strain of k_2 (bimorph) and is proportional to

$$z = x_2 - x_1$$

Subtracting (b-6) from (b-5), accordingly, gives the transducer response:

$$z = x_2 - x_1 = \frac{X_0 \left(\omega / \omega_{22} \right)^2}{\left[1 - \left(\frac{\omega}{\omega_{11}}\right)^2\right]\left[1 - \left(\frac{\omega}{\omega_{22}}\right)^2\right] - \frac{k_2}{k_1}} \qquad 6.$$

Assume that $k_1 \gg k_2$ that is, the fixture-armature stiffness is much greater than the bimorph stiffness. Equation 6 then becomes

$$z = \frac{X_0 \left(\omega \quad \omega_{22} \right)^2}{\left[1 - \left(\frac{\omega}{\omega_{11}}\right)^2\right]\left[1 - \left(\frac{\omega}{\omega_{22}}\right)^2\right]}$$

so that the transducer sensitivity function is then

$$\frac{V}{a} = S_D = \frac{K_D}{\left(1 - \frac{\omega^2}{\omega_{11}^2}\right)\left(\omega_{22}^2 - \omega^2\right)} \qquad 7.$$

where ω_{11} is the fixture-armature natural frequency and ω_{22} is the transducer natural frequency as measured on the calibrator.

The frequency ω_{11} may be determined by solving Equation 7 for the constant K and by evaluating the equation for two test runs corresponding to two different frequencies:

$$K_D = \left(1 - \frac{\omega_1^2}{\omega_{11}^2}\right)\left(\omega_{22}^2 - \omega_1^2\right) S_1$$

$$K_D = \left(1 - \frac{\omega_2^2}{\omega_{11}^2}\right)\left(\omega_{22}^2 - \omega_2^2\right) S_2 \qquad 7a.$$

These equations can be solved simultaneously for the two unknowns K and ω_{11}.

5.4 Correction Factor

It is seen from Equations 7 and 3a the correction factor is obtained from

$$\frac{S_D}{S_s} = 1 = \frac{K_D}{\left[1-\left(\frac{\omega}{\omega_{11}}\right)^2\right]\left[1-\left(\frac{\omega}{\omega_{22}}\right)^2\right]} \times \frac{1-\left(\frac{\omega}{\omega_{22}}\right)^2}{K_s}$$

or $$K_D = K_s\left[1-\left(\frac{\omega}{\omega_{11}}\right)^2\right] \qquad 8.$$

where K_s is the parameter calculated assuming a single-degree-of-freedom system.

Because it is impossible to avoid parasitic systems from being present in the calibration system it is interesting to examine the degree of stiffness required to shift the parasitic system frequency to a sufficient magnitude so that its effect will be tolerable. This can be done by solving Equation 8 for ω_{11}:

$$\omega_{11} = \frac{\omega}{\left(1 - \frac{K_D}{K_s}\right)^{1/2}}$$

where $$1 \geq \frac{K_D}{K_s} > 0$$

If 0.5% is tolerable for the calculation of K_s, the ratio K_D/K_s would be 0.955 and ω_{11} would have to be not lower than 14.14 or for $\omega = 6H_z$, $_{11}$ would be 84.85 H_z which is easily obtainable in structures such as used in

the calibrator system.

It is of interest to examine the influence of error in the determination of the parasitic frequency on the calculation of the piezoelectric constant K.

From Equation 7

$$K_D = S_D\left(1 - \frac{\omega^2}{\omega_{11}^2}\right)\left(\omega_{22}^2 - \omega^2\right) \qquad 9.$$

Referring to the quantities in the right-hand side of Equation 9 let only ω_{11} vary. Then

$$dK_D = S_D\left(\omega_{22}^2 - \omega^2\right)\left(2\frac{\omega^2}{\omega_{11}^3}\right) d\omega_{11}$$

Dividing by Equation 9 gives

$$\frac{dK_D}{K_D} = 2\frac{\omega^2}{\omega_{11}^2\left(1 - \frac{\omega^2}{\omega_{11}^2}\right)} \frac{d\omega_{11}}{\omega_{11}}$$

$$\left[\begin{array}{l}\text{Fractional}\\ \text{error in K}\end{array}\right] = \frac{2}{\left(\frac{\omega_{11}}{\omega}\right)^2 - 1} \times \left[\begin{array}{l}\text{Fractional}\\ \text{error in } \omega_{11}\end{array}\right]$$

It is seen that the higher the natural frequency of the parasitic oscillation the less important is the exactness in the measurement of its frequency. For example, if the parasitic is at 90 Hz $\pm$ 10% and ω is 6Hz

$$\frac{dK_D}{K_D} = \frac{2}{225 - 1} \times 0.1 \cong 9 \times 10^{-4} = 0.09\%$$

or the error in K will be 0.09%. However, if ω_{11} = 19.72 $\pm$ 10% and with ω = 6Hz,

$$\frac{dK_D}{K_D} = \frac{2}{10.8 - 1} \times 0.1 \cong 0.02 = 2\%$$

the error in K will be 2%.

5.5 Modification of the Calibrator

As a result of the parasitic oscillation study it was decided that the calibration system should be modified to remove the secondary mode by stiffening the armature, and by the re-positioning of the viewing index to a point closer to the mounting interface of the transducer.

Armature stiffening was accomplished by the use of light-weight trusses attached to the armature which greatly increased the armature area moment. The viewing point was moved to a position adjacent to the transducer mounting plate. The microscope vernier positioning table had to be moved to accommodate this new position.

Test runs indicated that the calibrator mounted transducer was now very close to being a single-degree-of-freedom system, and, thus, the simpler, more accurate, dynamical representation could be applied without need for the correction factor given above.

VI. TEMPERATURE SENSITIVITY STUDIES

Over the many years of the development of the falling sphere densitometer many temperature sensitivity investigations were performed both for the transducers and for the electronic system. Because at the outset of the present program there had been several changes in amplifier design and because periodic checking of the temperature stability of the bimorph piezoelectric ceramic is advisable it was decided to perform another temperature sensitivity study.

The temperature range of 50° to 90°F was selected which brackets the flight temperature range encountered of 60° to 80°F. Instead of using a standard chamber with its visual reading thermometer and the usual point-to-point recording of temperature vs voltage, and which does not lend itself conveniently to transducer measurements because of its vibrational environment (caused by pumps and fans), a special chamber was built with a quiescent heat source and which was provided with a bolometer temperature sensing circuit. This circuit provided an output voltage linear to ± .01% of the input temperature. The chamber was designed to fit around, but not touch, the transducer calibrator to expose the transducer under test to the controlled temperature environment.

The test sample was then excited at a constant amplitude, and at the start of each run its output was balanced out by means of an equal amplitude, equal frequency, but phase-opposed sinewave from a signal generator. The final output which was essentially at zero amplitude was placed on one channel of a recorder while the bolometer circuit output was placed on a second channel.

A heat sink block (aluminum) was cooled in a Tenny chamber to 40°F and then was placed in the test chamber. The test chamber heat source was enabled, and the recorder was started. The test chamber temperature was then allowed to slowly cover the range 50-90°F over a time interval of approximately two hours. Both transducers and amplifiers were tested in the same manner.

Temperature sensitivity was then determined by the broadening of the trace representing the output of the sample under test. A temperature sensitivity of the transducers of ± 0.05% was measured. No observable temperature sensitivity of the electronics was apparent.

Since temperature of the sphere changes only slightly from its launch temperature during its flight, it is felt that excellent performance with respect to temperature-caused error can be obtained by close control of the payload temperature on the pad, and then by launching when the payload is at the calibration temperature (usually 70°F).

VII. EVENT TIMER STUDY

The discrete power pulses for the initiation of the pyrotechnic squibs which separate the nose cone and eject the sphere from the rocket are generated by mechanical clock-work driven cams which activate micro-switches in series with the squib-bridge-wire-squib-battery circuit. The clock is started at launch by the action of first rocket motion on a mass-loaded pawl. The timer and battery pack are located in the mini-support unit.

These timers are procured from a sole-source vendor who intends to phase this product out of his line. They are still available but at greatly increased price and lead-time. As a result, an in-house research and development (IR&D-overhead funded) study was initiated to examine alternate systems to provide a more cost-effective means for generating the squib discretes.

Guidelines were established that only solid state electronic, non-mechanical methods would be examined because of their inherent low power, vibration-hardened, miniature, and low-cost characteristics. Digital counter type timers were found to have more precision, and therefore were more costly than required for the application. Attention was then focused on the capacitor run-down timer of the type used in the sphere for generating the caging-release squib discrete. This timer has been proven 100% reliable for eighteen rocket flights and for two satellite flights, and in all ground testing no failures have been encountered.

A system was evolved that used a simple piezoelectric acccelerometer of the compression type to sense the first motion acceleration of the rocket and thus produce a pulse to trigger the input of the run-down circuit. After a pre-set time interval the circuit would activate the nose-cone squib firing relay. This action would trigger another run-down circuit which

would, after another pre-set interval, activate the sphere-release squib firing relay.

It was found that the sphere power supply had ample energy margin over flight needs to fire the nose-cone and ejection squibs. A power buss would be required to pass from the sphere to the support unit via the sphere umbilical. This was found to be available by utilizing a spare terminal.

The elimination of the bulky mechanical timers and the squib battery packs from the mini-support unit enabled the reduction of its length from twelve inches to four inches. This length is constrained by the size of the main umbilical connector from the launcher.

VII. FIELDING

Four field trips were made during the course of the program:

1. Serial No. AC-15, TRACER, Wallops Island, VA, in June 1982
2. Serial No. AC-16, CAMP, Kiruna, Sweden, in July 1982
3. Serial No. AC-17, STATE, Poker Flat, Alaska in June 1983
4. Serial Nos. AC-18 and AC-8, MAPWINE, Andoya, Norway in December 1983 and January 1984

Payload preparation and pre-launch support was provided at all locations. Launch support was provided at all locations except Norway.

In all these operations preparations and check-out went according to plan except with payload AC-16 which developed an intermittent open circuit in its TM transmitter. This was readily corrected by replacement with a new transmitter.

All launches were nominal and yielded all sought-after scientific data.

END

FILMED

7-85

DTIC